Quaternary Science Reviews 28 (2009) 1625–1630

Contents lists available at ScienceDirect

Quaternary Science Reviews

journal homepage: www.elsevier.com/locate/quascirev

Geochemical constraints on the Laurentide Ice Sheet contribution to Meltwater Pulse 1A

Anders E. Carlson*

Department of Geology & Geophysics, University of Wisconsin, Madison, WI 53706, USA

ARTICLE INFO

Article history:
Received 9 September 2008
Received in revised form
8 January 2009
Accepted 4 February 2009

ABSTRACT

Planktonic and benthic $\delta^{18}O$ records adjacent to the runoff outlets of the Laurentide Ice Sheet (LIS) indicate that the LIS contributed to the abrupt ∼20 m rise in sea level ∼14.6 ka, Meltwater Pulse 1A (MWP-1A). However, the magnitude of the LIS contribution still remains unresolved. Here, I use a freshwater runoff–ocean mixing model to calculate the LIS meltwater required to explain the decreases in planktonic and benthic $\delta^{18}O$ observed during MWP-1A at the southern, eastern and northern runoff outlets of the LIS. Maximum LIS contributions in equivalent sea level rise for a 500-year long MWP-1A are 2.7 m discharged into the Gulf of Mexico as a combined hyperpycnal and hypopycnal flow, 2.1 m discharged into the North Atlantic, and 0.5 m into the Arctic Ocean, for a total LIS contribution of ≤5.3 m. A LIS contribution of <30% to MWP-1A supports the hypothesis that a significant component of this MWP was sourced from the Antarctic Ice Sheet.

1. Introduction

Meltwater Pulse 1A (MWP-1A) occurred ∼14.6 ka and is an ∼20 m rise in sea level in <500 years (Fairbanks, 1989; Bard et al., 1990; Edwards et al., 1993; Hanebuth et al., 2000). Due to its large size, the Laurentide Ice Sheet (LIS) was originally assumed to be the sole source of MWP-1A (Fairbanks, 1989; Peltier, 1994). However, LIS margin reconstructions show relatively small margin retreat during MWP-1A (Fig. 1) and steady state ice sheet models suggest that only a fraction of this meltwater pulse was sourced from the LIS (Clark et al., 1996; Licciardi et al., 1998, 1999; Dyke, 2004), which implies a large contribution from the Antarctic Ice Sheet (Clark et al., 1996). Sea-level fingerprinting and earth model studies suggest that an Antarctic source could account for ∼75% of the total sea level rise (Clark et al., 2002a; Bassett et al., 2005), although some LIS contribution cannot be excluded (Bassett et al., 2005).

Supporting a significant LIS contribution, one ice sheet modeling study reconstructed 8–10 m of MWP-1A coming from the LIS (Tarasov and Peltier, 2005, 2006), but still less than the LIS contribution of ∼16.5 m in the ICE-5G model (Peltier, 2004, 2005). This large ICE-5G LIS contribution would cause a 0.36–0.38 Sverdrup (Sv, $10^6\ m^3\ s^{-1}$) increase in LIS meltwater discharge during the course of the event. During MWP-1A, LIS meltwater was routed to the ocean via three outlets, the southern outlet (Mississippi River) to the Gulf of Mexico, the eastern outlet (Hudson and St. Lawrence Rivers) to the North Atlantic, and the northern outlet (Mackenzie River) to the Arctic Ocean (Fig. 1) (Licciardi et al., 1999; Tarasov and Peltier, 2005). Because a 0.36–0.38 Sv freshwater flux would force a reduction in Atlantic meridional overturning circulation (AMOC) strength (Stouffer et al., 2006) and AMOC increased during MWP-1A (Boyle and Keigwin, 1987; Weaver et al., 2003; McManus et al., 2004; Robinson et al., 2005), Tarasov and Peltier (2005, 2006) hypothesized that the meltwater discharged through the southern and eastern outlets (Fig. 1) entered the ocean as a dense, sediment laden, hyperpycnal flow along the ocean floor, which would presumably not affect AMOC. Note, however, that general circulation model simulations suggest that the southern outlet can only accommodate less than 6 m of sea level rise equivalent discharged as a hyperpycnal flow without reducing AMOC strength (Roche et al., 2007).

Reworked nannofossil records suggest increased southern outlet discharge during MWP-1A (Marchitto and Wei, 1995). Similarly, benthic foraminifera records from the Gulf of Mexico show a 0.9–2.3‰ decrease in $\delta^{18}O$ during MWP-1A (Fig. 2e), reflecting the input of ^{18}O-depleted terrestrial runoff and meltwater, and indicating that some portion of the LIS contribution entered the ocean as a hyperpycnal flow (Aharon, 2006). In contrast, grain size and sedimentation rate records from the eastern outlet indicate decreased sediment discharge, arguing against a hyperpycnal flow through the eastern outlet during MWP-1A (Keigwin and Jones, 1995). Nevertheless, there is a 0.69‰ light planktonic $\delta^{18}O$ anomaly observed adjacent to the eastern outlet at

* Corresponding author. Tel.: +1 608 262 1921.
E-mail address: acarlson@geology.wisc.edu

0277-3791/$ – see front matter
doi:10.1016/j.quascirev.2009.02.011

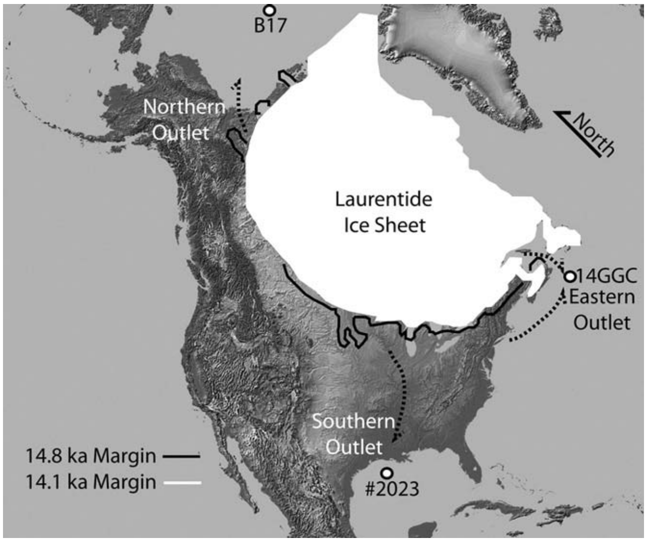

Fig. 1. Map of the Laurentide Ice Sheet extent ∼14.1 ka (white line filled in) with the additional area covered by ice at ∼14.8 ka indicated by the black solid lines (Dyke, 2004). Core locations are indicated by black and white dots; LOUIS Core #2023 (#2023) (27.76°N, 92.59°W, 401 m water depth) (Aharon, 2006), OCE3326-14GGC (14GGC) (43.07°N, 55.83°W, 3525 m water depth) (Keigwin et al., 2005), and 94B-17 (B17) (81.27°N, 178.97°W, 2217 m water depth) (Poore et al., 1999; Hall and Chan, 2004). Dashed lines indicate freshwater routing directions to the southern, eastern and northern outlets.

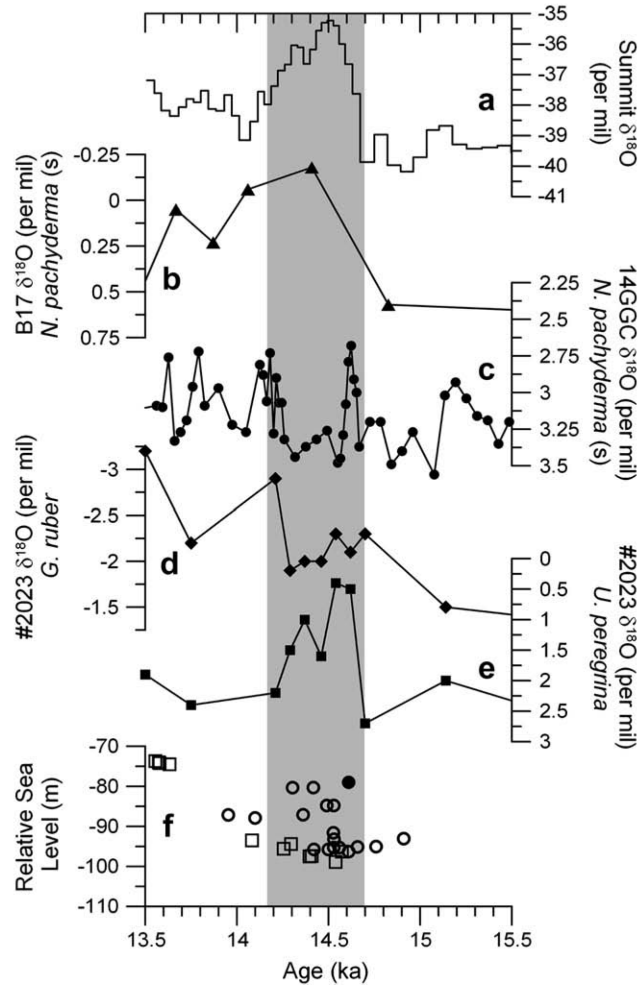

Fig. 2. Deglacial runoff records (see Fig. 1), GISP2 temperature and relative sea level. (a) GISP2 $\delta^{18}O$ (Grootes et al., 1993). (b) $\delta^{18}O$ of *N. pachyderma* (s) recording runoff to the northern outlet (B17, triangles) (Poore et al., 1999; Hall and Chan, 2004). (c) *N. pachyderma* (s) $\delta^{18}O$ recording runoff to the eastern outlet (14GGC, circles) (Keigwin et al., 2005). (d) *G. ruber* $\delta^{18}O$ recording hypopycnal runoff through the southern outlet (#2023, diamonds) (Aharon, 2003, 2006). (e) *U. peregrina* $\delta^{18}O$ recording hyperpycnal runoff to the southern outlet (#2023, squares) (Aharon, 2006). (f) Relative sea level data; open squares corals from Barbados (Bard et al., 1990; Peltier and Fairbanks, 2006), open circles mangroves from Sunda Shelf (Hanebuth et al., 2000), and solid circles corals from Huon Peninsula (Edwards et al., 1993). The $\delta^{18}O$ records are presented on their original published, calibrated age models. Gray bar denotes the timing of Meltwater Pulse 1A.

∼14.5 ka, suggesting increased freshwater discharge or warming during MWP-1A (Fig. 2c) (Keigwin et al., 2005). A 0.75‰ decrease in planktonic $\delta^{18}O$ in the Arctic Ocean has been correlated with MWP-1A and indicates increased discharge through the northern outlet (Poore et al., 1999; Hall and Chan, 2004) (Fig. 2b). In contrast, iceberg discharge from the LIS into the Labrador Sea decreased and planktonic $\delta^{18}O$ increased during MWP-1A implying that the northeastern LIS did not contribute significantly to this MWP (Andrews and Tedesco, 1992; Clark et al., 1996; Hillaire-Marcel and Bilodeau, 2000).

Here, I use a freshwater runoff-ocean mixing model to determine the amount of LIS meltwater and thus the LIS contribution to MWP-1A through the southern, eastern and northern outlets recorded by these light planktonic and benthic $\delta^{18}O$ anomalies (Figs. 1 and 2). Assuming that no temperature adjustments are necessary (see Section 3), these records suggest increased runoff from the LIS during part or all of MWP-1A through the main outlets. This analysis indicates, however, that the contribution from the LIS was only a small fraction (<30%) of the total sea level rise during MWP-1A, suggesting that the LIS was not the primary source of this MWP.

2. Methods and results

A freshwater runoff-ocean mixing model is employed to calculate the amount of meltwater from the LIS required to explain the decreases in $\delta^{18}O$ at the various runoff outlets (Aharon, 2003, 2006; Carlson et al., 2007). The $\delta^{18}O$ of runoff (δ_r) (combined ice melt and precipitation–evaporation (P-E)) is calculated as Eq. (1):

$$\delta_{r-x} = \frac{f_{p-x} \times \delta_p + f_{i-x} \times \delta_i}{f_{p-x} + f_{i-x}} \tag{1}$$

where $f_{p\text{-}x}$ (Sv) is the flux of P-E and δ_p its $\delta^{18}O$, and $f_{i\text{-}x}$ (Sv) is the flux of LIS meltwater and δ_i its $\delta^{18}O$, at time step x ($x = 1$ for pre-MWP-1A, $x = 2$ for during MWP-1A). With the exception of the southern outlet records (see below), $f_{p\text{-}x}$ is considered constant for both time steps (Licciardi et al., 1999). Prior to MWP-1A, $f_{i\text{-}1}$ is derived from Licciardi et al. (1999), with the exception of the southern outlet benthic record. During MWP-1A, $f_{i\text{-}2}$ is the model-tuned parameter. δ_p and δ_i are considered constants. The mixture $\delta^{18}O$ at the core site ($\delta_{m\text{-}x}$) at time x is calculated as Eq. (2):

$$\delta_{m-x} = \frac{f_o \times \delta_o + \left(f_{p-x} + f_{i-x}\right) \times \delta_{r-x}}{f_o + f_{p-x} + f_{i-x}} \tag{2}$$

where f_o (Sv) is the ocean flux and δ_o the ocean $\delta^{18}O$. Eq. (3) is used to determine the $\Delta\delta^{18}O$ observed during MWP-1A:

$$\Delta\delta^{18}o = \delta_{m-2} - \delta_{m-1} \tag{3}$$

with subscripts m-2 and m-1 indicating the δ_m during MWP-1A ($x = 2$) and before MWP-1A ($x = 1$). The model is forced by varying $f_{i\text{-}2}$ in Eqs. (1) and (2) in the time step during MWP-1A ($x = 2$) so that the solution to Eq. (3) matches the observed $\Delta\delta^{18}O$ in the records (Fig. 2). This assumes that during MWP-1A the P-E discharge (f_p) and ocean flux (f_o) did not change, the temperature of the water masses did not change, and the $\delta^{18}O$ of P-E (δ_p) and ice melt (δ_i) did not change. The effects of these assumptions are discussed in Section 3.

End member fluxes (f) and $\delta^{18}O$ (δ) are derived from the literature. For δ_i, two end members are used that span the range of estimates, −25‰ derived from western Canadian plains porewater injected by the LIS (Remenda et al., 1994) and −35‰ derived from considerations of LIS mass balance (Aharon, 2003). The other flux (f) and $\delta^{18}O$ (δ) values are listed in Table 1 along with their literature sources. In the case of the Southern Outlet benthic record prior to MWP-1A, $f_{p\text{-}1}$ and $f_{i\text{-}1} = 0$ Sv, because the site is bathed completely in ocean water prior to the hyperpycnal discharge (Aharon, 2006). During MWP-1A, $f_{p\text{-}2}$ increases to 0.0856 Sv for modeling the benthic record (Licciardi et al., 1999). In the case of the Southern Outlet planktonic record, $f_{p\text{-}1} = 0.1157$ Sv and $f_{i\text{-}1} = 0.0164$ Sv prior to MWP-1A, and $f_{p\text{-}2} = 0.030$ Sv during MWP-1A (Licciardi et al., 1999). The benthic and planktonic $f_{p\text{-}2}$ values during MWP-1A are calculated using a total southern outlet $f_{p\text{-}2}$ of 0.1157 Sv (Licciardi et al., 1999) and partitioning this between hyperpycnal and hypopycnal entry based on the relative contribution of the benthic (−2.3‰) and planktonic (−0.8‰) records to the combined $\Delta\delta^{18}O$ anomaly of −3.1‰ (Fig. 2d,e, Table 1). Varying the partitioning between hyperpycnal and hypopycnal entry does not change the total amount LIS meltwater discharged through the southern outlet during MWP-1A.

Model results are shown in Fig. 3. The southern outlet benthic anomaly of −2.30‰ (Fig. 2e) requires a 0.020–0.014 Sv increase in LIS meltwater for a δ_i of −25‰ and −35‰, respectively (Fig. 3a). This is equivalent to 0.9–0.6 m of sea level rise in 500 years. The southern outlet planktonic anomaly of −0.80‰ (Fig. 2d) requires 0.042–0.032 Sv increase for δ_i of −25‰ and −35‰, respectively (Fig. 3b). This is equivalent to 1.8–1.4 m of sea level rise in 500 years. The combined LIS MWP-1A contribution through the southern outlet is 2.7–2.0 m equivalent sea level rise in 500 years (Fig. 4). The eastern outlet planktonic anomaly of −0.69‰ (Fig. 2c) requires 0.049–0.045 Sv increase for δ_i of −25‰ and −35‰, respectively (Fig. 3c). This is equivalent to 2.1–2.0 m of sea level rise in 500 years (Fig. 4). The northern outlet planktonic anomaly of −0.75‰ (Fig. 2b) requires 0.011–0.009 Sv increase for δ_i of −25‰

Table 1
End member fluxes (f) and $\delta^{18}O$ (δ) used in the model (Eqs. (1)–(3)) for the Southern Outlet benthic (SO_B) and planktonic (SO_P) records, the Eastern Outlet (EO) planktonic record and the Northern Outlet (NO) planktonic record

Outlet	f_o	δ_o	δ_p	$f_{p\text{-}1}$	$f_{p\text{-}2}$	$f_{i\text{-}1}$
SO_B[a,b]	0.476	1.7	−7.7	0.0000	0.0856	0.0000
SO_P[a,b]	0.159	1.7	−7.7	0.1157	0.0300	0.0164
EO[b,c,d,e]	0.739	0.0	−10.0	0.0617	0.0617	0.0067
NO[b,d,f,g]	0.158	−2.0	−20.0	0.0272	0.0272	0.0037

Values are derived from the literature.
[a] Aharon (2003, 2006).
[b] Licciardi et al. (1999).
[c] Dickie and Trites (1983).
[d] LeGrande and Schmidt (2006).
[e] Yang et al. (1996).
[f] Hall and Chan (2004).
[g] MacDonald et al. (1989).

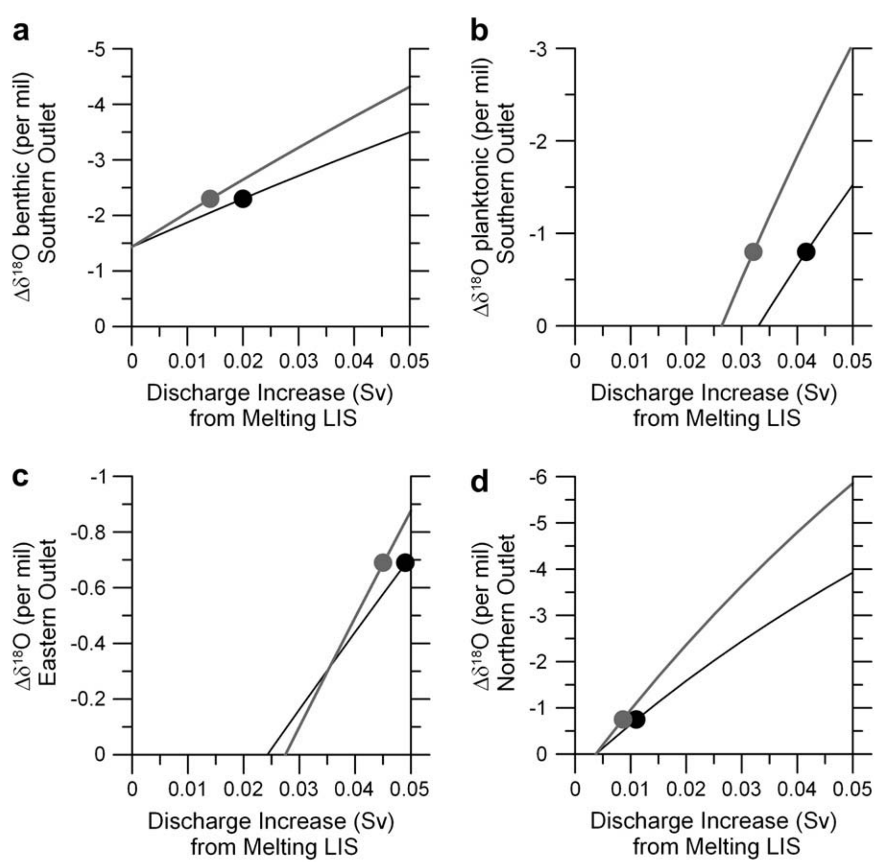

Fig. 3. Modeled $\Delta\delta^{18}O$ versus increased Laurentide Ice Sheet (LIS) meltwater discharge (Sverdrups, Sv, 10^6 m^3 s^{-1}). Black line for a δ_i end member of −25‰ (Remenda et al., 1994), gray line for a δ_i end member of −35‰ (Aharon, 2003). Symbols indicate the discharge increase from LIS melting to explain the observed $\Delta\delta^{18}O$ excursion (Fig. 2). (a) Southern Outlet benthic model. (b) Southern Outlet planktonic model. (c) Eastern Outlet planktonic model. (d) Northern Outlet planktonic model.

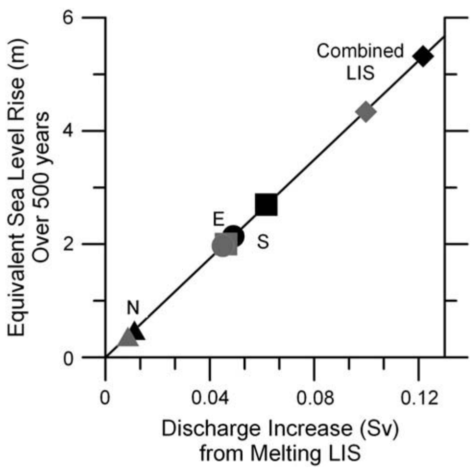

Fig. 4. Relationship between increased Laurentide Ice Sheet melting (Sv) and its contribution to sea level rise (m) over a 500-year period. Squares are combined hyperpycnal and hypopycnal discharge for the Southern Outlet (S). Triangles are the Northern Outlet (N). Circles are the Eastern Outlet (E). Diamonds are the combined LIS contribution. Black symbols are for a −25‰ δ_i LIS end member, gray symbols are for a −35‰ δ_i LIS end member.

and −35‰, respectively (Fig. 3d). This is equivalent to 0.5–0.4 m of sea level rise in 500 years (Fig. 4).

3. Discussion and conclusions

The combined LIS contribution to MWP-1A recorded in these records is 5.3–4.4 m of equivalent sea level rise in 500 years, for the δ_i end member of −25‰ and −35‰, respectively (Fig. 4). This range depends, however, on several of the assumptions in model end member values. The LIS meltwater δ^{18}O values (δ_i) may have been outside the range of −25 to −35‰. Indeed, Fairbanks (1989) suggested a LIS δ^{18}O of −42‰, which would reduce the LIS MWP-1A contribution to ∼4.0 m of equivalent sea level rise.

Another assumption is that P-E amounts (f_p) did not change during MWP-1A. Presumably, the abrupt warming of the North Atlantic region into the Bølling warm period (Fig. 2a) may have increased P. However, this increase may have been partially offset by increased E as suggested by general circulation models (Kutzbach et al., 1998; Licciardi et al., 1999). Increasing P-E (f_p) would decrease the amount of LIS meltwater (f_i) required to explain the light δ^{18}O anomalies, reducing the LIS MWP-1A contribution. For instance, a doubling of P-E (f_p) coincident with Bølling warming and MWP-1A would reduce the LIS contribution to ∼3.2 m of equivalent sea level rise, with the benthic southern outlet and planktonic northern outlet δ^{18}O anomalies completely explained by the increase in P-E.

Similarly, the ocean water flux (f_o) was likely different from the modern flux during MWP-1A, which will change the estimated LIS sea level rise contribution. Any reduction in the ocean flux will only decrease the LIS discharge amount required to explain the observed $\Delta\delta^{18}$O, and thus reduce the LIS MWP-1A contribution. Increased ocean fluxes will increase the required LIS discharge amount. A doubling of the ocean fluxes (f_o) relative to modern (Table 1) would increase the LIS MWP-1A contribution to 8.8 and 6.9 m of sea level equivalent for δ_i end member of −25‰ and −35‰, respectively. However, AMOC and its shallow return flow were likely reduced relative to present during the last deglaciation (Boyle and Keigwin, 1987; McManus et al., 2004; Schmidt et al., 2004; Robinson et al., 2005; Came et al., 2008) suggesting that LIS MWP-1A contributions through the southern and eastern outlets based on modern ocean fluxes are maximum estimates. The Arctic Ocean flux for the northern outlet is likely the least well constrained (Poore et al., 1999; Hall and Chan, 2004). Note that the northern outlet transported the least amount of meltwater discharge (Fig. 3d) (doubling the ocean flux only increases the sea level equivalent volume through this outlet by 0.1–0.2 m). Furthermore, the Bering Strait did not open until ∼11 ka (i.e., Keigwin et al., 2006), well after MWP-1A, implying a reduced Arctic Ocean flux relative to modern during MWP-1A and thus a maximum flux estimate using the modern ocean flux.

In using the observed $\Delta\delta^{18}$O from the records, the competing effect of water temperature on foraminifera δ^{18}O was not considered. The effect of regional warming into the Bølling warm period (Fig. 2a) as AMOC strength increased (Clark et al., 2002b; McManus et al., 2004) would cause a decrease in foraminifera δ^{18}O reducing the actual LIS meltwater component in the δ^{18}O anomaly. In the case of the southern outlet benthic record, this effect is likely minimal given the small temperature changes that occur in benthic environments (Aharon, 2006). Similarly, the northern outlet record in the Arctic Ocean probably experienced little sea surface temperature (SST) warming (Poore et al., 1999; Hall and Chan, 2004). However, SST changes may have affected the planktonic records from the southern and eastern outlets. For the southern outlet, an adjacent *G. ruber* SST record suggests relatively constant SST during MWP-1A (Flower et al., 2004). In contrast, planktonic foraminifera counts from the eastern outlet show an ∼60% reduction in polar species (*N. pachyderma* (s)) during MWP-1A (Keigwin and Jones, 1995) implying 3–4 °C warming of the mixed layer (Hilbrecht, 1996). Dynoflagellate cyst reconstructions also suggest a 4–5 °C SST increase near the eastern outlet (deVernal et al., 1996). The mixed layer 3–4 °C warming could account for all of the observed δ^{18}O decrease, making the modeled LIS meltwater contribution to MWP-1A through the eastern outlet a maximum estimate.

While there is evidence that 0.9–0.6 m of the LIS contribution to MWP-1A entered the ocean as a hyperpycnal flow through the southern outlet, whether this phenomenon occurred at the eastern and northern outlets remains untested by benthic δ^{18}O records. However, Tarasov and Peltier (2005) argued that hyperpycnal flows would be unlikely to occur into the Arctic Ocean because of sea ice formation, making it improbable that additional meltwater entered the ocean through this outlet undetected by the planktonic foraminifera. As previously noted, grain size and sedimentation records from the eastern outlet indicate a reduction in grain size and sedimentation rates during MWP-1A suggesting minimal freshwater input through the eastern outlet via a sediment laden, hyperpycnal flow (Keigwin and Jones, 1995). Therefore, while there may still be an unaccounted for LIS contribution to MWP-1A entering as hyperpycnal flows through the eastern and northern outlets, it is probably not a significant portion of MWP-1A.

The larger increase in LIS meltwater discharge (f_i) indicated by the southern outlet planktonic record compared to the benthic record (Fig. 3a,b) despite a larger decrease in benthic δ^{18}O (Fig. 2d,e) is due to the amount of freshwater runoff reaching the habitat of the foraminifera species prior to MWP-1A. Prior to MWP-1A, the δ^{18}O of the surface water mass (habitat of *G. ruber*) at the core site (#2023) (Fig. 1) was a mixture of ocean water and continental runoff (P-E and meltwater) (Aharon, 2003, 2006; Flower et al., 2004). In contrast, the benthic (*U. peregrina*) δ^{18}O record is relatively constant except for the large decrease in δ^{18}O during MWP-1A suggesting that the bottom water mass did not receive freshwater runoff prior to MWP-1A (Aharon, 2006). The introduction of freshwater runoff (P-E and meltwater) to the benthic water mass during MWP-1A has a larger impact on the resulting mixed $\Delta\delta^{18}$O than would occur if the water mass was already receiving some freshwater runoff (see Eqs. (1)–(3)), explaining this apparent discrepancy.

The combined hyperpycnal and hypopycnal discharge from LIS meltwater of 0.062–0.046 Sv through the southern outlet is significantly less than that modeled by Aharon (2006) for the same $\Delta\delta^{18}O$ excursions in the same core. The Aharon (2006) discharge increase of 0.33–0.28 Sv integrates over 500 years to a LIS MWP-1A contribution of 14.4–12.2 m of equivalent sea level rise through the southern outlet if this discharge is assumed to be entirely from the melting LIS. The difference between these two estimates is due to the choice of the southern outlet freshwater runoff $\delta^{18}O$ (δ_r). Aharon (2006) assumed a constant combined freshwater runoff $\delta^{18}O$ (δ_r) of −9.8 to −11‰ using a fixed ratio of the ice melt (f_i) and P-E (f_p) contributions to the total freshwater runoff and thus a fixed runoff $\delta^{18}O$ (δ_r). The Aharon (2006) fixed δ_r values (−9.8 to −11‰) were calculated with a LIS δ_i of −25 and −35‰, respectively, assuming 88% of the freshwater runoff was constantly derived from P-E (f_p) and only 12% from LIS melting (f_i). Consequently only 12% of the 0.33–0.28 Sv increase calculated by Aharon (2006) is from the melting LIS (the remaining 88% is due to increased P-E). Because increased P-E does not affect sea level, the actual LIS MWP-1A contribution through the southern outlet from the estimates of Aharon (2006) is 1.7–1.4 m of equivalent sea level rise. Indeed, inserting constant δ_r values of −9.8 to −11‰ into Eq. (2) produces similar results as Aharon (2006). Here, P-E (f_p) is considered constant with the $\Delta\delta^{18}O$ excursions attributed solely to LIS melting (maximum sea level rise contribution, see above). Thus δ_r varies with the amount of LIS meltwater added to the total freshwater runoff ($f_{i\text{-}2} + f_{p\text{-}2}$, Eq. (1)), which produces a lower δ_r and requires less total freshwater runoff to explain the $\Delta\delta^{18}O$ excursions. This method also produces a larger LIS MWP-1A contribution through the southern outlet than the Aharon (2006) estimates (2.7–2.0 m vs. 1.7–1.4 m) after accounting for the Aharon (2006) assumption of a constant ratio for the P-E (f_p) and meltwater (f_i) contributions to the total freshwater runoff.

The total LIS contribution of 5.3–4.4 m of equivalent sea level rise suggests the LIS contributed <30% of the ∼20 m of sea level rise during MWP-1A (Fig. 2f), which is a maximum contribution, given that the assumptions that went into the model are conservative in design. Assuming a 500-year duration for MWP-1A, the $\Delta\delta^{18}O$-based reconstruction is at least ∼11 m and ∼5 m less than the ICE-5G reconstruction (Peltier, 2004) and the ice sheet model of Tarasov and Peltier (2005, 2006), respectively. The $\Delta\delta^{18}O$-based reconstruction is in better agreement with steady-state ice sheet models and the LIS margin record history. The Licciardi et al. (1998) steady-state ice sheet model reconstructed LIS sea level rise contributions of 6.6–5.6 m between 15.4 and 14.0 ka, slightly higher than the $\Delta\delta^{18}O$-based reconstruction, but note the longer time interval (∼1400 years vs. 500 years) in the Licciardi et al. reconstruction. To directly compare the $\Delta\delta^{18}O$-based reconstruction and the LIS margin record, I converted LIS area (A_i, km^2) (Fig. 1) (Dyke, 2004) to LIS volume (V_i, km^3) using the relationship developed for ice sheets and ice caps (Paterson, 1994):

$$log(V_i) = 1.23 \times [log(A_i) - 1] \quad (4)$$

Although Eq. (4) assumes an ice sheet in equilibrium, it was developed from ice sheets and ice caps in both negative and positive mass balance states. These ice sheets and ice caps span 4 orders of magnitude in area (Antarctic Ice Sheet to Barnes Ice Cap) and climate conditions from maritime (Iceland) to polar desert (Antarctica). This results in an error of ∼12%. The LIS area lost between ∼14.8 and 14.1 ka (Fig. 1) suggests a LIS contribution of 4.3 ± 0.5 m of equivalent sea level rise in agreement with the $\Delta\delta^{18}O$-based reconstruction.

The significantly smaller LIS MWP-1A contribution, and thus freshwater discharge, in the $\Delta\delta^{18}O$-based reconstruction than in other reconstructions (i.e., Peltier, 2004, 2005; Tarasov and Peltier, 2005, 2006) helps explain why AMOC strength increased concurrent with MWP-1A (Boyle and Keigwin, 1987; Weaver et al., 2003; McManus et al., 2004; Robinson et al., 2005). This $\Delta\delta^{18}O$-based reconstruction is also in agreement with sea-level fingerprinting and earth model studies that suggest ∼25% of MWP-1A came from Northern Hemisphere Ice Sheets (Clark et al., 2002a; Bassett et al., 2005). In contrast, Peltier (2004, 2005) and Tarasov and Peltier (2005, 2006) hypothesized that the other Northern Hemisphere ice sheets (Barents-Kara, Scandinavian and Cordilleran Ice Sheets) contributed a combined 8–10 m to MWP-1A. The deglacial chronologies of these ice sheets do not, however, support this hypothesis. The southern margin of the Scandinavian Ice Sheet retreated less than 100 km during MWP-1A (Rinterknecht et al., 2006). Similarly, planktonic and benthic $\delta^{18}O$ records from the Norwegian Sea suggest a reduction in freshwater discharge during MWP-1A relative to earlier meltwater discharge from the Scandinavian Ice Sheet (Lehman et al., 1991; Karpuz and Jansen, 1992; Clark et al., 1996). The much smaller Cordilleran Ice Sheet also retreated only a relatively small distance during MWP-1A when compared to later retreat (Dyke, 2004). The major retreat and melt-back of the Barents-Kara Ice Sheet occurred ∼18–17 ka, well before MWP-1A leaving significantly less ice available at ∼14.6 ka to contribute to MWP-1A (Jones and Keigwin, 1988; Koç and Jansen, 1994; Svendsen et al., 2004).

In conclusion, I note that the $\Delta\delta^{18}O$-based reconstruction rules out any large LIS contribution to MWP-1A and supports earlier paleoclimate-based arguments for a small LIS contribution (Clark et al., 1996). This $\Delta\delta^{18}O$-based LIS MWP-1A contribution contains several assumptions (no change in temperature, P-E, or ocean circulation) that are conservative in design and thus the 5.3 m of sea level rise from the LIS should be viewed as a maximum estimate with the possibility of a significantly smaller contribution to MWP-1A. Therefore, a significant component of MWP-1A was likely sourced from the Antarctic Ice Sheet.

Acknowledgements

The author would like to thank L. Keigwin for sharing data and P. Clark for providing comments on the initial manuscript. Comments and suggestions by R. Stevenson and an anonymous reviewer improved this manuscript. A.E.C. is supported by University of Wisconsin-Madison start-up funds and the National Science Foundation Paleoclimate Program.

References

Aharon, P., 2003. Meltwater flooding events in the Gulf of Mexico revisited: implications for rapid climate changes during the last deglaciation. Paleoceanography 18, doi:10.1029/2002PA000840.
Aharon, P., 2006. Entrainment of meltwaters in hyperpycnal flows during deglaciation superfloods in the Gulf of Mexico. Earth and Planetary Sciences 241, 260–270.
Andrews, J.T., Tedesco, K., 1992. Detrital carbonate-rich sediments, northwestern Labrador Sea: implications for ice-sheet dynamics and iceberg rafting (Heinrich) events in the North Atlantic. Geology 20, 1087–1090.
Bard, E., Hamelin, B., Fairbanks, R.G., Zindler, A., 1990. Calibration of the ^{14}C timescale over the past 30,000 years using mass spectrometric U–Th ages from Barbados corals. Nature 345, 405–410.
Bassett, S.E., Milne, G.A., Mitrovica, J.X., Clark, P.U., 2005. Ice sheet and solid earth influences on far-field sea-level histories. Science 309, 925–928.
Boyle, E.A., Keigwin, L.D., 1987. North Atlantic thermohaline circulation during the past 20,000 years linked to high-latitude surface temperature. Nature 330, 35–40.
Came, R.E., Oppo, D.W., Curry, W.B., Lynch-Stieglitz, J., 2008. Deglacial variability in the surface return flow of the Atlantic meridional overturning circulation. Paleoceanography 23, 2438–2441. 10.129/2007PA001450.
Carlson, A.E., Clark, P.U., Haley, B.A., Klinkhammer, G.P., Simmons, K., Brook, E.J., Meissner, K.J., 2007. Geochemical proxies of North American freshwater routing

during the Younger Dryas cold event. Proceedings of the National Academy of Sciences USA 104, 6556–6561.
Clark, P.U., Alley, R.B., Keigwin, L.D., Licciardi, J.M., Johnsen, S., Wang, H., 1996. Origin of the first global meltwater pulse following the last glacial maximum. Paleoceanography 11, 563–577.
Clark, P.U., Mitrovica, J.X., Milne, G.A., Tamisiea, M.E., 2002a. Sea-level fingerprinting as a direct test for the source of global meltwater Pulse IA. Science 295, 2438–2441.
Clark, P.U., Pisias, N.G., Stocker, T.F., Weaver, A.J., 2002b. The role of the thermohaline circulation in abrupt climate change. Nature 415, 863–869.
deVernal, A., Hillaire-Marcel, C., Bilodeau, G., 1996. Reduced meltwater outflow from the Laurentide ice margin during the Younger Dryas. Nature 381, 774–777.
Dickie, L.M., Trites, R.W., 1983. The Gulf of St. Lawrence. In: Ketchum, B.W. (Ed.), Ecosystems of the World 26, Estuaries and Enclosed Seas. Elsevier, New York, pp. 403–425.
Dyke, A.S., 2004. An outline of North American deglaciation with emphasis on central and northern Canada. In: Ehlers, J., Gibbard, P.L. (Eds.), Quaternary Glaciations: Extent and Chronology. Elsevier, Amsterdam, pp. 373–424.
Edwards, R.L., Beck, J.W., Burr, G.S., Donahue, D.J., Chappell, J.M.A., Bloom, A.L., Druffel, E.R.M., Taylor, F.W., 1993. A large drop in atmospheric $^{14}C/^{12}C$ and reduced melting in the Younger Dryas, documented with ^{230}Th ages of corals. Science 260, 962–968.
Fairbanks, R.G., 1989. A 17,000-year glacio-eustatic sea level record: influence of glacial melting rates on the Younger Dryas event and deep-ocean circulation. Nature 342, 637–642.
Flower, B.P., Hastings, D.W., Hill, H.W., Quinn, T.M., 2004. Phasing of deglacial warming and Laurentide Ice Sheet meltwater in the Gulf of Mexico. Geology 32, 597–600.
Grootes, P.M., Stuiver, M., White, J.W.C., Johnsen, S., Jouzel, J., 1993. Comparison of oxygen isotope records from the GISP2 and GRIP Greenland ice cores. Nature 366, 552–554.
Hall, J.M., Chan, L.-H., 2004. Ba/Ca in *Neogloboquadrina pachyderma* as an indicator of deglacial meltwater discharge into the western Arctic Ocean. Paleoceanography 19, doi:10.1029/2003PA000910.
Hanebuth, T., Stattegger, K., Grootes, P.M., 2000. Rapid flooding of the Sunda Shelf: a late-glacial sea-level record. Science 288, 1033–1035.
Hilbrecht, H., 1996. Extant planktic foraminifera and the physical environment in the Atlantic and Indian Oceans. Mitteilungen aus dem Geologischen Institut der Eidgen. Technischen Hochschule und der Universität Zürich, Neue Folge. No. 300, Zurich, Austria, 93 pp.
Hillaire-Marcel, C., Bilodeau, G., 2000. Instabilities in the Labrador Sea water mass structure during the last climatic cycle. Canadian Journal of Earth Science 37, 795–809.
Jones, G.A., Keigwin, L.D., 1988. Evidence from Fram Strait (78° N) for early deglaciation. Nature 336, 56–59.
Karpuz, N.A., Jansen, E., 1992. A high-resolution diatom record of the last deglaciation from the southeast Norwegian Sea: documentation of rapid climatic changes. Paleoceanography 7, 499–520.
Keigwin, L.D., Jones, G.A., 1995. The marine record of deglaciation from the continental margin off Nova Scotia. Paleoceanography 10, 973–985.
Keigwin, L.D., Sachs, J.P., Rosenthal, Y., Boyle, E.A., 2005. The 8200 year B.P. event in the slope water system, western subpolar North Atlantic. Paleoceanography 20, doi:10.1029/2004PA001074.
Keigwin, L.D., Donnelly, J.P., Cook, M.S., Driscoll, N.W., Brigham-Grette, J., 2006. Rapid sea-level rise and Holocene climate in the Chukchi Sea. Geology 34, 861–864.
Koç, N., Jansen, E., 1994. Response of the high-latitude Northern Hemisphere to orbital climate forcing: evidence from the Nordic Seas. Geology 22, 523–526.
Kutzbach, J., Gallimore, R., Harrison, S., Behling, P., Selin, R., Laarif, F., 1998. Climate and biome simulations for the past 21,000 years. Quaternary Science Reviews 17, 473–506.
LeGrande, A.N., Schmidt, G.A., 2006. Global gridded data set of the oxygen isotopic composition in seawater. Geophysical Research Letters 33, doi:10.1029/2006GL026011.
Lehman, S.J., Jones, G.A., Keigwin, L.D., Andersen, E.S., Butenko, G., 1991. Initiation of Fennoscandian ice sheet retreat during the last deglaciation. Nature 349, 513–516.
Licciardi, J.M., Clark, P.U., Jenson, J.W., MacAyeal, D.R., 1998. Deglaciation of a soft-bedded Laurentide Ice Sheet. Quaternary Science Reviews 17, 427–448.
Licciardi, J.M., Teller, J.T., Clark, P.U., 1999. Freshwater routing by the Laurentide ice sheet during the last deglaciation. In: Clark, P.U., Webb, R.S., Keigwin, L.D. (Eds.), Mechanisms of Global Climate Change at Millennial Time Scales. Geophysical Monthly Series, No. 112. American Geophysical Union, pp. 177–201.
MacDonald, R.W., Carmack, E.C., McLaughlin, F.A., Iseki, K., MacDonald, D.M., O'Brien, M.C., 1989. Composition and modification of water masses in the Mackenzie Shelf Estuary. Journal of Geophysical Research 94, 18057–18070.
Marchitto, T.M., Wei, K.-Y., 1995. History of Laurentide meltwater flow to the Gulf of Mexico during the last deglaciation, as revealed by reworked calcareous nannofossils. Geology 23, 779–782.
McManus, J.F., Francois, R., Gherardi, J.-M., Keigwin, L.D., Brown-Leger, S., 2004. Collapse and rapid resumption of Atlantic meridional circulation linked to deglacial climate changes. Nature 428, 834–837.
Paterson, W.S.B., 1994. The Physics of Glaciers. Butterworth-Heinemann, Oxford, 480 pp.
Peltier, W.R., 1994. Ice age paleotopography. Science 265, 195–201.
Peltier, W.R., 2004. Global glacial isostasy and the surface of the ice-age Earth: the ICE-5G (VM2) model and GRACE. Annual Reviews of Earth and Planetary Sciences 32, 111–149.
Peltier, W.R., 2005. On the hemispheric origins of meltwater pulse 1a. Quaternary Science Reviews 24, 1655–1671.
Peltier, W.R., Fairbanks, R.G., 2006. Global glacial ice volume and last glacial maximum duration from an extended Barbados sea level record. Quaternary Science Reviews 25, 3322–3337.
Poore, R.Z., Osterman, L., Curry, W.B., Phillips, R.L., 1999. Late Pleistocene and Holocene meltwater events in the western Arctic Ocean. Geology 27, 759–762.
Remenda, V.H., Cherry, J.A., Edwards, T.W.D., 1994. Isotopic composition of old ground water from Lake Agassiz: implications for Late Pleistocene climate. Science 266, 1975–1978.
Rinterknecht, V.R., Clark, P.U., Raisbeck, G.M., Yiou, F., Bitnas, A., Brook, E.J., Marks, L., Zelcs, V., Lunkka, J.-P., Pavlovskaya, I.E., Piotrowski, J.A., Raukas, A., 2006. The last deglaciation of the southeastern sector of the Scandinavian Ice Sheet. Science 311, 1449–1452.
Robinson, L.F., Adkins, J.F., Keigwin, L.D., Southon, J., Fernandez, D.P., Wang, S.-L., Scheirer, D.S., 2005. Radiocarbon variability in the western North Atlantic during the last deglaciation. Science 310, 1469–1473.
Roche, D., Renssen, H., Weber, S.L., Goosse, H., 2007. Could meltwater pulses have been sneaked unnoticed into the deep ocean during the last glacial? Geophysical Research Letters 34, doi:10.1029/2007GL032064.
Schmidt, M.W., Spero, H.J., Lea, D.W., 2004. Links between salinity variation in the Caribbean and North Atlantic thermohaline circulation. Nature 428, 160–163.
Stouffer, R.J., et al., 2006. Investigating the causes of the response of the thermohaline circulation to past and future climate changes. Journal of Climate 19, 1365–1387.
Svendsen, J.I., Gataullin, V., Mangerud, J., Polyak, L., 2004. The glacial history of the Barents and Kara Sea region. In: Ehlers, J., Gibbard, P.L. (Eds.), Quaternary Glaciations: Extent and Chronology. Elsevier, Amsterdam, pp. 369–378.
Tarasov, L., Peltier, W.R., 2005. Arctic freshwater forcing of the Younger Dryas cold reversal. Nature 435, 662–665.
Tarasov, L., Peltier, W.R., 2006. A calibrated deglacial drainage chronology for the North American continent: evidence of an Arctic trigger for the Younger Dryas. Quaternary Science Review 25, 659–688.
Weaver, A.J., Saenko, O.A., Clark, P.U., Mitrovica, J.X., 2003. Meltwater Pulse 1A from Antarctica as a trigger of the Bølling-Allerød warm interval. Science 299, 1709–1713.
Yang, C., Telmer, K., Veizer, J., 1996. Chemical dynamics of the "St. Lawrence" riverine system: δD_{H2O}, $\delta^{18}O_{H2O}$, $\delta^{13}C_{DIC}$, $\delta^{34}S_{sulfate}$, and dissolved $^{87}Sr/^{86}Sr$. Geochimica et Cosmochimica Acta 60, 851–866.